

General Properties on Applying the Principle of Minimum Sensitivity to High-order Perturbative QCD Predictions

Yang Ma, Xing-Gang Wu,^{*} Hong-Hao Ma, and Hua-Yong Han

*Department of Physics, Chongqing University, Chongqing 401331, P.R. China and
Institute of Theoretical Physics, Chongqing University, Chongqing 401331, P.R. China*

(Dated: September 20, 2021)

As one of the key components of perturbative QCD theory, it is helpful to find a systematic and reliable way to set the renormalization scale for a high-energy process. The conventional treatment is to take a typical momentum as the renormalization scale, which assigns an arbitrary range and an arbitrary systematic error to pQCD predictions, leading to the well-known renormalization scheme and scale ambiguities. As a practical solution for such scale setting problem, the “Principle of Minimum Sensitivity” (PMS), has been proposed in the literature. The PMS suggests to determine an optimal scale for the pQCD approximant of an observable by requiring its slope over the scheme and scale changes to vanish. In the paper, we present a detailed discussion on general properties of PMS by utilizing three quantities $R_{e^+e^-}$, R_τ and $\Gamma(H \rightarrow b\bar{b})$ up to four-loop QCD corrections. After applying the PMS, the accuracy of pQCD prediction, the pQCD convergence, the pQCD predictive power and etc., have been discussed. Furthermore, we compare PMS with another fundamental scale setting approach, i.e. the Principle of Maximum Conformality (PMC). The PMC is theoretically sound, which follows the renormalization group equation to determine the running behavior of coupling constant and satisfies the standard renormalization group invariance. Our results show that PMS does provide a practical way to set the effective scale for high-energy process, and the PMS prediction agrees with the PMC one by including enough high-order QCD corrections, both of which shall be more accurate than the prediction under the conventional scale setting. However, the PMS pQCD convergence is an accidental, which usually fails to achieve a correct prediction of unknown high-order contributions with next-to-leading order QCD correction only, i.e. it is always far from the “true” values predicted by including more high-order contributions.

PACS numbers: 12.38.Bx, 12.38.Aw, 11.15.Bt

I. INTRODUCTION

According to the renormalization group (RG) invariance [1–6], a physical observable should not depend on any “unphysical” choices. In another words, the RG-invariance indicates that the dependence of an observable on the renormalization scheme and scale should vanish. However, for fixed-order pQCD approximations, the renormalization scheme and scale dependence from both the running coupling and the corresponding expansion coefficients at the same order do not exactly cancel. To deal with a fixed-order calculation, one usually takes the renormalization scale as the typical momentum transfer of the process, or a value to minimize the contributions of large loop diagrams, and varies it over a certain range to ascertain its uncertainty. This conventional scale setting procedure leads to well-known renormalization scheme and scale ambiguities and assigns an arbitrary range and an arbitrary systematic error to fixed-order pQCD predictions. To solve such renormalization scheme and scale ambiguities, it is helpful to find a general way to set the optimal scale and hence the optimal running behavior of strong coupling constant for any processes via a process-independent and systematic way, cf. a recent review on QCD scale setting [7].

To compare with the conventional scale setting, it has been suggested by Stevenson at 1981 that one can achieve a good prediction for an observable by requiring its pQCD approximant to be minimum sensitive to the variations of those unphysical parameters. This treatment is called as the “Principle of Minimum Sensitivity (PMS)” [8–10]. The PMS admits that different scheme and scale choices do lead to theoretical uncertainties, however the “true” prediction of an observable can only be achieved by using optimal scheme and scale. The scheme dependence of the PMS predictions have been analyzed in Refs.[11, 12]. It is noted that the PMS satisfies local RG-invariance [13], which provides a practical approach to systematically fix the optimal scheme and scale for high-energy process. It has been noted that after applying the PMS, the pQCD prediction does show a fast steady behavior over the scheme and scale changes. As an example, it has been applied to study the fixed-point behavior of the coupling constant at the low-energy region [14, 15].

On the other hand, it has also been observed that PMS does not satisfy the RG-properties such as symmetry, reflexivity, and transitivity [16]. So the relations among different physical observables depend on the choice of intermediate renormalization scheme, leading to residual scheme dependence. Moreover, the predicted PMS scale for three-jet production via e^+e^- -annihilation can not yield correct physical behavior at the next-to-leading order (NLO) level, i.e. it anomalously rises without bound

^{*} email:wuxg@cqu.edu.cn

for small jet energy [17, 18]. There are even doubts on the usefulness of PMS [19]. All those discussions indicate the necessity of further careful studies on theoretical principles underlying the PMS and on applications to more high-loop examples.

Great improvements on understanding the PMS procedures and on applying PMS scale setting to higher perturbative orders other than the NLO level have recently been achieved in Ref.[20]. In recent years, there are many progresses on studying the two-loop and higher QCD corrections. For examples, the quantities $R_{e^+e^-}$, R_τ and $\Gamma(H \rightarrow b\bar{b})$ have been calculated up to four-loop level under the $\overline{\text{MS}}$ -scheme [21–24]. With all those developments, it is possible to make a detailed discussion on general properties of PMS, and to show to what degree it can be applied. For the purpose, we shall present the PMS predictions for $R_{e^+e^-}$, R_τ and $\Gamma(H \rightarrow b\bar{b})$ up to four-loop level. General PMS properties, such as the accuracy of the pQCD prediction, the convergence of the perturbative series, the predictive power of pQCD theory and etc, shall be discussed via comparing the predictions with those under the conventional scale setting.

Recently, another well-known scale setting approach, i.e. the Brodsky-Lepage-Mackenzie approach suggested by Brodsky et al. at 1983 [25], has been developed into a fundamental one, i.e. the “Principle of Maximum Conformality (PMC)” [26–32]. In different to PMS scale setting, the PMC states that we should determine different optimal scales for the high-energy process under different schemes, and the final predictions are independent on the scheme choices due to commensurate scale relations [33] and also the scheme-independence of a conformal series. The running behavior of the coupling constant is governed by the RG-equation [34–40]. Inversely, the PMC states the optimal behavior/scale of the coupling constant can be achieved by using the β -terms in perturbative series. The PMC follows standard RG-invariance and satisfies all RG-properties [16]. When one applies the PMC, the scales of the coupling constant are shifted at each order such that no contributions proportional to the QCD β -function remain. The resulting pQCD series is thus identical to a scheme-independent conformal series. Since the resulting series is free of divergent renormalon terms [41, 42], the pQCD convergence can be naturally improved. The PMS and PMC scale settings have quite different starting points and their predictions usually have quite different perturbative nature, it is thus helpful to present a detailed comparison of the PMS predictions with the PMC ones.

The remaining parts of the paper are organized as follows. In Sec.II we first present a short review on local RG-invariance that underlies PMS, then, we present the PMS formulas up to high-perturbative orders. A tricky way to derive the PMS RG-invariants at high-orders in the Appendix. In Sec.III we investigate the PMS properties based on three quantities $R_{e^+e^-}$, R_τ and $\Gamma(H \rightarrow b\bar{b})$ up to four-loop level. In Sec.IV we present a detailed comparison of PMS and PMC via the quantity $R_{e^+e^-}$.

Sec.V is reserved for a summary.

II. CALCULATION TECHNOLOGY FOR THE PMS SCALE SETTING

Conventionally, the running behavior of the strong coupling constant is controlled by the following $\beta^{\mathcal{R}}$ -function or the RG-equation,

$$\beta^{\mathcal{R}} = \mu^2 \frac{\partial}{\partial \mu^2} \left(\frac{\alpha_s^{\mathcal{R}}(\mu)}{4\pi} \right) = - \sum_{i=0}^{\infty} \beta_i^{\mathcal{R}} \left(\frac{\alpha_s^{\mathcal{R}}(\mu)}{4\pi} \right)^{i+2}, \quad (1)$$

where μ stands for the renormalization scale, and the superscript \mathcal{R} stands for an arbitrary renormalization scheme (usually taken as the $\overline{\text{MS}}$ -scheme). For convenience and without introducing any confusion, we shall omit the superscript \mathcal{R} in the following formulas. The first two β -terms, $\beta_0 = 11 - \frac{2}{3}n_f$ and $\beta_1 = 102 - \frac{38}{3}n_f$, are scheme independent, where n_f is the number of active flavors; while the β_n -terms with ($n \geq 2$) are scheme dependent [36–40]. The scheme dependence/transformation for high-order β -terms have been discussed in Refs.[43–45].

It is convenient to use $\tau = \ln(\mu^2/\tilde{\Lambda}_{\text{QCD}}^2)$ and $\beta_{n \geq 2}$ to label a particular choice of renormalization scale and renormalization scheme [8]. Here $\tilde{\Lambda}_{\text{QCD}}$ is the reduced asymptotic scale, which is defined as

$$\tilde{\Lambda}_{\text{QCD}} = \left(\frac{\beta_1}{\beta_0^2} \right)^{-\beta_1/2\beta_0^2} \Lambda_{\text{QCD}}. \quad (2)$$

We can study the scale- and scheme- dependence of the pQCD predictions via the extended RG-equations [8, 46].

A. Local RG-invariance and PMS

As an illustration of local RG-invariance, we deal with the perturbative approximant (ϱ_n) for an arbitrary physical observable ϱ , which can be written as

$$\varrho_n(Q) = \mathcal{C}_0(Q) a_s^p(\mu) + \sum_{i=1}^n \mathcal{C}_i(Q, \mu) a_s^{i+p}(\mu), \quad (3)$$

where Q is the experimental scale at which it is measured, $a_s = \alpha_s/\pi$, and p is the power of coupling constant associated with tree-level term. The calculation of the coefficients \mathcal{C}_i involves ultraviolet divergences which must be regulated and removed by a renormalization procedure. At the finite order, the pQCD predictions dependent on the choice of renormalization scheme and scale, i.e.

$$\partial \varrho_n / \partial (\text{RS}) = \mathcal{O}(a_s^{p+n}), \quad (4)$$

where RS stands for the scheme or scale parameter, respectively. Eq.(4) shows the self-consistency of a perturbation theory, i.e. the N^{th} -LO approximate ϱ_n must agree to $\mathcal{O}(a_s^{p+n})$ under different choices of scheme and scale.

The tree-level coefficient \mathcal{C}_0 is scheme and scale independent, we set its value to be 1 in later calculations. When $\mathcal{C}_0 \neq 1$, the results can be obtained via the transformation, $\mathcal{C}_i(Q, \mu) \rightarrow \mathcal{C}'_i(Q, \mu) = \mathcal{C}_i(Q, \mu)/\mathcal{C}_0$.

As mentioned in the Introduction, there are renormalization scheme and scale ambiguities for the fixed-order pQCD approximant ϱ_n . The PMS suggests to eliminate such scheme and scale ambiguities by finding optimal scheme and optimal scale of the process, which can be

achieved by requiring ϱ_n to satisfy the following equations [8, 20],

$$\frac{\partial \varrho_n}{\partial \tau} = 0, \quad (5)$$

$$\frac{\partial \varrho_n}{\partial \beta_m} = 0. \quad (m = 2, \dots, n) \quad (6)$$

They can be further written as

$$\frac{\partial \varrho_n}{\partial \tau} = \left(\frac{\partial}{\partial \tau} \Big|_{a_s} + \beta(a_s) \frac{\partial}{\partial (a_s/4)} \right) \varrho_n = 0, \quad (7)$$

$$\frac{\partial \varrho_n}{\partial \beta_m} = \left(\frac{\partial}{\partial \beta_m} \Big|_{a_s} - \beta(a_s) \int_0^{a_s/4} d\left(\frac{a'_s}{4}\right) \frac{(a'_s/4)^{m+2}}{[\beta(a'_s)]^2} \frac{\partial}{\partial (a_s/4)} \right) \varrho_n = 0, \quad (m = 2, 3, \dots) \quad (8)$$

where the integration in the second equations can be

treated via the α_s -expansion,

$$\beta(a_s) \int_0^{a_s/4} d\left(\frac{a'_s}{4}\right) \frac{(a'_s/4)^{m+2}}{[\beta(a'_s)]^2} = -\frac{(a_s/4)^{j+1}}{\beta_0} \left(\frac{1}{j-1} - \frac{\beta_1}{\beta_0} \frac{j-2}{j(j-1)} \left(\frac{a_s}{4}\right) + \dots \right).$$

The standard RG-invariance states that only the physical observable $\varrho = \varrho_n|_{n \rightarrow \infty}$ agrees with those equations. Thus, using Eqs.(7,8) for the fixed-order approximant is theoretically unsound, and they instead introduce a kind of local RG-invariance [13]. This provides the reason why the PMS does not satisfy the basic RG-properties [16]. The PMS, however, provides an intuitive way to set the optimal scheme and optimal scale, and its resultant tends to be steady over the scheme and scale changes around the optimal point.

The running behavior of strong coupling constant can be obtained via solving RG-equation (1), which can be rewritten as

$$\begin{aligned} \tau &= \int_{a_s/4}^{\infty} d\left(\frac{x}{4}\right) \frac{1}{\beta^{(n)}(x)} \\ &= \frac{4}{\beta_0 a_s} + \frac{\beta_1}{\beta_0^2} \ln \left| \frac{\beta_1 a_s}{\beta_1 a_s + 4\beta_0} \right| + \Delta(a_s), \end{aligned} \quad (9)$$

where

$$\Delta(a_s) = \int_0^{a_s/4} d\left(\frac{x}{4}\right) \left(\frac{1}{\beta^{(n)}(x)} - \frac{1}{\beta^{(1)}(x)} \right). \quad (10)$$

The symbol $\beta^{(n)}$ stands for the cut β -function up to a_s^{n+2} . Eq.(9) is the “integrated β -function equation”, or simply, the “int- β equation”, which can be solved numerically.

In the following, we shall show how PMS applies local RG-invariance to set the optimal scale and how the RG-invariant coefficients at each order are derived.

B. PMS procedures up to high-orders

For a N^{th} -LO pQCD approximate (3), we have to fix totally $2n+1$ variables for determining optimal scheme and optimal scale, i.e. $\tilde{a}_s, \tilde{\tau}, \tilde{\beta}_2, \dots, \tilde{\beta}_n, \tilde{\mathcal{C}}_1, \dots, \tilde{\mathcal{C}}_n$. Those parameters can be fixed by using n local RG-equations (7,8), one int- β equation (9), and also n scheme-and-scale independent RG-invariants from the self-consistency relation (4). To be a useful reference for applying PMS scale setting, we take the QCD corrections up to N^3 -LO level as a detailed explanation.

At the NLO level, the NLO approximate is

$$\varrho_1 = a_s^p (1 + \mathcal{C}_1 a_s).$$

The NLO approximate ϱ_1 can be calculated in an initial choice of scheme (usually the $\overline{\text{MS}}$ -scheme) and scale. We have three parameters $\tilde{a}_s, \tilde{\tau}$ and $\tilde{\mathcal{C}}_1$ to be determined.

Differentiating ϱ_1 over τ and using the self-consistency relation (4), i.e. the coefficient at the order of $\mathcal{O}(a_s^{p+1})$ should be zero, we obtain

$$\frac{\partial \mathcal{C}_1}{\partial \tau} = \frac{1}{4} p \beta_0. \quad (11)$$

Integrating it over τ , we get one RG-invariant integration constant ρ_1 , which can be expressed as

$$\rho_1 = \frac{1}{4} p \beta_0 \tau - \mathcal{C}_1 = \frac{1}{4} p \beta_0 \tilde{\tau} - \tilde{\mathcal{C}}_1, \quad (12)$$

where the second equation is from the RG invariance. As a tricky point, since ρ_1 depends solitarily on Q at which the observable is measured, one can transform $\varrho_n(Q)$ as $\varrho_n(\rho_1)$. The advantage of such transformation lies in that, $\varrho_n(\rho_1)$ does not depend on Λ_{QCD} , thus avoiding the uncertainties from the choice of Λ_{QCD} .

From Eq.(7), we obtain the NLO local RG-equation

$$p\beta_0 - [p\tilde{a}_s^{p-1} + (p+1)\tilde{C}_1\tilde{a}_s^p] \left(\beta_0 + \frac{\beta_1\tilde{a}_s}{4} \right) = 0, \quad (13)$$

which leads to

$$\tilde{C}_1 = -\frac{p\beta_1}{(p+1)(4\beta_0 + \beta_1\tilde{a}_s)}. \quad (14)$$

Together with the NLO int- β equation

$$\tilde{\tau} = \frac{4}{\beta_0\tilde{a}_s} + \frac{\beta_1}{\beta_0^2} \ln \left| \frac{\beta_1\tilde{a}_s}{\beta_1\tilde{a}_s + 4\beta_0} \right|, \quad (15)$$

we finally obtain

$$\frac{1}{\tilde{a}_s} + \frac{p\beta_1}{(p+1)(4\beta_0 + \beta_1\tilde{a}_s)} + \frac{\beta_1}{4\beta_0} \ln \left| \frac{\beta_1\tilde{a}_s}{\beta_1\tilde{a}_s + 4\beta_0} \right| = \not{16} \quad (16)$$

From those equations (14,15,16), we can derive $\tilde{\tau}$, \tilde{C}_1 , \tilde{a}_s , and finally the get optimized prediction for ϱ_1 .

For high-order QCD corrections, we can apply similar procedures via a step-by-step way for determining all the parameters.

Using the self-consistency condition (4), the local RG invariants ρ_n can be determined via an order-by-order way. Once a ρ_n has been determined at a particular perturbative order, it shall be fixed for all high-order PMS treatment. Except for those local RG invariants, all other parameters should be re-determined when new high-order corrections are included.

At the N²-LO level, we have five parameters to be determined, i.e. \tilde{a}_s , $\tilde{\tau}$, β_2 , \tilde{C}_1 , and \tilde{C}_2 . There are two equations that can be obtained from the local RG-equations $\partial\varrho_2/\partial\tau = 0$ and $\partial\varrho_2/\partial\beta_2 = 0$:

$$16(2+p)\tilde{C}_2\beta_0 + 4 \left[(1+p)\tilde{C}_1 + (2+p)\tilde{C}_2\tilde{a}_s \right] \beta_1 + \left[\tilde{a}_s \left(\tilde{C}_1 + 2\tilde{C}_2\tilde{a}_s \right) + p \left(1 + \tilde{C}_1\tilde{a}_s + \tilde{C}_2\tilde{a}_s^2 \right) \right] \tilde{\beta}_2 = 0, \quad (17)$$

$$48 \left[(1+p)\tilde{C}_1 + (2+p)\tilde{C}_2\tilde{a}_s \right] \beta_0 + \tilde{a}_s \left[\tilde{a}_s \left(\tilde{C}_1 + 2\tilde{C}_2\tilde{a}_s \right) + p \left(1 + \tilde{C}_1\tilde{a}_s + \tilde{C}_2\tilde{a}_s^2 \right) \right] \tilde{\beta}_2 = 0. \quad (18)$$

At the N³-LO level, we have seven parameters to be determined, i.e. \tilde{a}_s , $\tilde{\tau}$, $\tilde{\beta}_2$, $\tilde{\beta}_3$, \tilde{C}_1 , \tilde{C}_2 , and \tilde{C}_3 . There

are three local RG-equations that can be obtained from $\partial\varrho_3/\partial\tau = 0$, $\partial\varrho_3/\partial\beta_2 = 0$, and $\partial\varrho_3/\partial\beta_3 = 0$:

$$64(3+p)\tilde{C}_3\beta_0 + 16 \left((2+p)\tilde{C}_2 + (3+p)\tilde{C}_3\tilde{a}_s \right) \beta_1 + 4 \left((1+p)\tilde{C}_1 + \tilde{a}_s \left((2+p)\tilde{C}_2 + (3+p)\tilde{C}_3\tilde{a}_s \right) \right) \tilde{\beta}_2 + \left(p + \tilde{C}_1\tilde{a}_s + p\tilde{C}_1\tilde{a}_s + 2\tilde{C}_2\tilde{a}_s^2 + p\tilde{C}_2\tilde{a}_s^2 + (3+p)\tilde{C}_3\tilde{a}_s^3 \right) \tilde{\beta}_3 = 0, \quad (19)$$

$$384 \left[(2+p)\tilde{C}_2 + (3+p)\tilde{C}_3\tilde{a}_s \right] \beta_0^2 - \tilde{a}_s \left\{ p \left(1 + \tilde{C}_1\tilde{a}_s + \tilde{C}_2\tilde{a}_s^2 + \tilde{C}_3\tilde{a}_s^3 \right) + \tilde{a}_s \left[\tilde{C}_1 + \tilde{a}_s \left(2\tilde{C}_2 + 3\tilde{C}_3\tilde{a}_s \right) \right] \right\} \beta_1\tilde{\beta}_2 + \left\{ p \left(1 + \tilde{C}_1\tilde{a}_s + \tilde{C}_2\tilde{a}_s^2 + \tilde{C}_3\tilde{a}_s^3 \right) + \tilde{a}_s \left[\tilde{C}_1 + \tilde{a}_s \left(2\tilde{C}_2 + 3\tilde{C}_3\tilde{a}_s \right) \right] \right\} \beta_0 \left(8\tilde{\beta}_2 + 3\tilde{a}_s\tilde{\beta}_3 \right) = 0, \quad (20)$$

$$96 \left\{ (1+p)\tilde{C}_1 + \tilde{a}_s \left[(2+p)\tilde{C}_2 + (3+p)\tilde{C}_3\tilde{a}_s \right] \right\} \beta_0^2 - 8 \left\{ p \left(1 + \tilde{C}_1\tilde{a}_s + \tilde{C}_2\tilde{a}_s^2 + \tilde{C}_3\tilde{a}_s^3 \right) + \tilde{a}_s \left[\tilde{C}_1 + \tilde{a}_s \left(2\tilde{C}_2 + 3\tilde{C}_3\tilde{a}_s \right) \right] \right\} \beta_0\beta_1 + \tilde{a}_s \left\{ p \left(1 + \tilde{C}_1\tilde{a}_s + \tilde{C}_2\tilde{a}_s^2 + \tilde{C}_3\tilde{a}_s^3 \right) + \tilde{a}_s \left[\tilde{C}_1 + \tilde{a}_s \left(2\tilde{C}_2 + 3\tilde{C}_3\tilde{a}_s \right) \right] \right\} \beta_1^2 = 0. \quad (21)$$

Up to N³-LO level, in addition to ρ_1 , we need to determine two extra RG invariants ρ_2 and ρ_3 , which can be fixed via a similar way as the NLO case, detailed procedures can be found in Refs.[13, 20, 47]. Then, we obtain

$$\rho_2 = \mathcal{C}_2 - \frac{(1+p)\mathcal{C}_1^2}{2p} - \frac{\beta_1\mathcal{C}_1}{4\beta_0} + \frac{p\beta_2}{16\beta_0} \quad (22)$$

$$= \tilde{\mathcal{C}}_2 - \frac{(1+p)\tilde{\mathcal{C}}_1^2}{2p} - \frac{\beta_1\tilde{\mathcal{C}}_1}{4\beta_0} + \frac{p\tilde{\beta}_2}{16\beta_0} \quad (23)$$

and

$$\rho_3 = 2\mathcal{C}_3 + \frac{\mathcal{C}_1^2\beta_1}{4p\beta_0} - \frac{\mathcal{C}_1\beta_2}{8\beta_0} + \frac{p\beta_3}{64\beta_0} + \frac{2(1+p)(2+p)\mathcal{C}_1^3}{3p^2} - \frac{2(2+p)\mathcal{C}_1\mathcal{C}_2}{p} \quad (24)$$

$$= 2\tilde{\mathcal{C}}_3 + \frac{\tilde{\mathcal{C}}_1^2\tilde{\beta}_1}{4p\beta_0} - \frac{\tilde{\mathcal{C}}_1\tilde{\beta}_2}{8\beta_0} + \frac{p\tilde{\beta}_3}{64\beta_0} + \frac{2(1+p)(2+p)\tilde{\mathcal{C}}_1^3}{3p^2} - \frac{2(2+p)\tilde{\mathcal{C}}_1\tilde{\mathcal{C}}_2}{p}. \quad (25)$$

The first equations (22,24) are to set the value of $\rho_{2,3}$ with the known parameters calculated under the initial scheme-and-scale choices, the second equations (23,25) are due to scheme-and-scale independence of RG-invariants $\rho_{2,3}$. As a cross-check of those formulas, when setting $p = 1$, we turn to the same expressions as those of Ref.[13, 20].

As a summary, in combination with all local RG-equations, the known RG-invariants, and also the same order int- β equation (9), we are ready to derive all the wanted optimal parameters. This can be done numerically by following the ‘‘spiraling’’ method [13, 48, 49]. For a general all-order determination, the procedures of the ‘‘spiraling’’ method are

- Firstly, one takes an initial value for \tilde{a}_s , which can be approximated by using RG-equation at the same order at an arbitrary initial scale. This initial scale should be large enough to ensure the pQCD calculation, which can be practically (to short the number of iterations) taken as the typical momentum flow of the process.
- Secondly, for the first iteration, one sets the initial values for the scheme-dependent $\tilde{\beta}_2, \dots, \tilde{\beta}_n$ to be β_2, \dots, β_n that have been calculated under an initial renormalization scheme. For new iterations their values are replaced by the ones determined from the last iteration. Then, one solves the local RG-equations, similar to Eqs.(13,17,18,19,20,21), for $\tilde{\mathcal{C}}_1, \dots, \tilde{\mathcal{C}}_n$.
- Thirdly, one applies the calculated value of $\tilde{\mathcal{C}}_1, \dots, \tilde{\mathcal{C}}_n$ into the equations on RG-invariants ρ_1, \dots, ρ_n , similar to Eqs.(12,23,25), for $\tilde{a}_s, \tilde{\tau}, \tilde{\beta}_2, \dots, \tilde{\beta}_n$.
- Finally, one iterates from second step until the results for ϱ_n converge to an acceptable prediction.

As a remarkable feature of renormalization theory, even if the coefficients \mathcal{C}_n and the β -terms β_n are separately different in different schemes, there exist some combinations of them that are RG-invariant. The above derived integration parameters ρ_n are such kind of RG-invariants, which are key components to determine the ‘‘optimal ϱ_n ’’. Because ρ_n are RG-invariants, one can demonstrate that the final PMS predictions are independent of any choice of initial scale, being consistent with one of requirement of basic RG-invariance [7]. Thus, to apply PMS, one can simply set the initial scale to be a typical one such as the typical momentum of the process or the one at which the observable is measured. This,

inversely, provides us a simpler/tricky way to derive the RG-invariants ρ_n , which are put in the Appendix.

III. GENERAL PROPERTIES AND APPLICATIONS OF PMS SCALE SETTING

In this section, we shall present a detailed discussion on general properties of PMS scale setting by utilizing three quantities $R_{e^+e^-}$, R_τ and $\Gamma(H \rightarrow b\bar{b})$ up to four-loop level. A comparison of PMS and conventional scale settings shall also be presented.

A. $R_{e^+e^-}$ up to four-loop QCD corrections

The e^+e^- annihilation provides one of the most precise tests of pQCD theory. Its measurable quantity, i.e. the R -ratio $R(Q)$, is defined as

$$\begin{aligned} R_{e^+e^-}(Q) &= \frac{\sigma(e^+e^- \rightarrow \text{hadrons})}{\sigma(e^+e^- \rightarrow \mu^+\mu^-)} \\ &= 3 \sum_q e_q^2 [1 + R(Q)], \end{aligned} \quad (26)$$

where Q stands for the e^+e^- collision energy at which the R -ratio is measured. The pQCD approximant for $R(Q)$ up to $(n+1)$ -loop correction can be written as

$$R_n(Q, \mu_0) = \sum_{i=0}^n \mathcal{C}_i(Q, \mu_0) a_s^{i+1}(\mu_0), \quad (27)$$

where μ_0 stands for an arbitrary initial scale and $a_s = \alpha_s/\pi$. Under the conventional scale setting, the renormalization scale shall be fixed to μ_0 ; while for a certain scale setting approach, the renormalization scale shall be varied from μ_0 to a certain degree.

The quantity $R_n(Q, \mu_0)$ has been calculated up to four-loop levels under the $\overline{\text{MS}}$ -scheme [21, 22], whose coefficients for $\mu_0 = Q$ read

$$\begin{aligned} \mathcal{C}_0 &= 1, \\ \mathcal{C}_1 &= 1.9857 - 0.1152n_f, \\ \mathcal{C}_2 &= -6.63694 - 1.20013n_f - 0.00518n_f^2 - 1.240\eta, \\ \mathcal{C}_3 &= -156.61 + 18.77n_f - 0.7974n_f^2 + 0.0215n_f^3, \end{aligned}$$

where $\eta = \left(\sum_q e_q\right)^2 / \left(3\sum_q e_q^2\right)$, n_f and e_q stand for the number and electric charge of the active flavors. Because of the factorial-growth of renormalon terms, the magnitude of the coefficient \mathcal{C}_i generally grows with the increment of QCD loops, providing the dominant source for

lessening the convergence of pQCD series. By applying the PMS, we shall show such kind of factorial growth can be softened to a certain degree.

To do the numerical calculation, the QCD parameter $\Lambda_{\overline{\text{MS}}}$ is fixed by using $\alpha_s(M_Z) = 0.1185 \pm 0.0006$ [50]. For self-consistency, the $\Lambda_{\overline{\text{MS}}}$ for R_n shall be determined by using $(n+1)$ -loop α_s -running determined from the RG-equation (1). For example, we obtain $\Lambda_{\overline{\text{MS}}}^{(n_f=5)} = 214$ MeV for R_3 by using four-loop α_s -running. Under the conventional scale setting, the renormalization scale shall be fixed to μ_0 ; while for the PMS, the renormalization scale shall be the optimal one determined from local RG-invariance. In the following discussions, if not specially stated, we shall take $\mu_0 = Q$.

	$n_f=3$	$n_f=4$	$n_f=5$
\mathcal{C}_1	1.6401	1.5249	1.4097
\mathcal{C}_2	-10.284	-11.6857	-12.8047
\mathcal{C}_3	-106.896	-92.9124	-80.0075
$\mathcal{C}_1^{\text{PMS}}$	-0.458	-0.1105	0.0479
$\mathcal{C}_2^{\text{PMS}}$	-1.1361	0.2103	1.3075
$\mathcal{C}_3^{\text{PMS}}$	32.2133	24.9881	16.4108

TABLE I. Coefficients for the perturbative expansion of $R_3(Q)$ before and after the PMS scale setting, where we have set $Q = 1.2$ GeV for $n_f=3$, $Q = 3$ GeV for $n_f=4$, and $Q = 31.6$ GeV for $n_f=5$.

The coefficients \mathcal{C}_1 , \mathcal{C}_2 and \mathcal{C}_3 before and after the PMS scale setting for various flavor numbers, i.e. $n_f = 3, 4$, and 5 , are presented in Table I. Three typical scales, $Q = 1.2$ GeV, 3 GeV, and 31.6 GeV, are adopted for various flavor numbers. After applying the PMS, the magnitude of the coefficients \mathcal{C}_i become smaller than those under the conventional scale setting, indicating that the divergent renormalon terms have been suppressed.

As for conventional scale setting, one usually takes the same renormalization scale for pQCD predictions up to any perturbative order. Then, under conventional scale setting, the effective coupling $\tilde{a}_s^{(n)} \equiv a_s^{(n)}$, and the slight differences among $\tilde{a}_s^{(n)}$ with various n are directly caused by the conventional α_s -behavior up to $(n+1)$ -loops.

	$n_f = 3$	$n_f = 4$	$n_f = 5$
$\tilde{a}_s^{(1)}(\text{Conv.})$	0.1414	0.0823	0.0450
$\tilde{a}_s^{(2)}(\text{Conv.})$	0.1320	0.0814	0.0450
$\tilde{a}_s^{(3)}(\text{Conv.})$	0.1370	0.0820	0.0450
$\tilde{a}_s^{(1)}(\text{PMS})$	0.2156	0.1052	0.0504
$\tilde{a}_s^{(2)}(\text{PMS})$	0.1265	0.0832	0.0464
$\tilde{a}_s^{(3)}(\text{PMS})$	0.1212	0.0819	0.0461

TABLE II. The effective coupling $\tilde{a}_s^{(n)}$ under the conventional (Conv.) and the PMS scale settings, where $n = 1, 2$, and 3 , respectively. Here we have set $Q = 1.2$ GeV for $n_f=3$, $Q = 3$ GeV for $n_f=4$, and $Q = 31.6$ GeV for $n_f=5$.

After applying the PMS, we shall have different effective/optimal coupling $\tilde{a}_s^{(n)}$ (PMS) for each R_n . The effective coupling $\tilde{a}_s^{(n)}$ for R_n under those two scale settings are shown in Table II, where $n = 1, 2$, and 3 , respectively. To determine the PMS effective coupling, one does not need to know the value of Λ_{QCD} , thus the uncertainties from Λ_{QCD} are eliminated¹. It is noted that the PMS effective coupling $\tilde{a}_s^{(n)}$ (PMS) becomes smaller for a larger n , i.e. $\tilde{a}_s^{(1)}$ (PMS) $>$ $\tilde{a}_s^{(2)}$ (PMS) $>$ $\tilde{a}_s^{(3)}$ (PMS). This agrees with the previous observation of Ref. [52] and is consistent with the ‘‘induced convergence’’ [53].

Next, we turn to numerical analysis of R_n under the PMS and conventional scale settings. For the purpose, we fix $Q = 31.6$ GeV, at which the R -ratio has been measured [54].

	LO	NLO	N ² LO	N ³ LO	total
Conv.	0.04499	0.00285	-0.00117	-0.00033	0.04635
PMS	0.04608	0.00010	0.00013	0.00007	0.04638

TABLE III. The LO, NLO, N²LO and N³LO loop contributions for the approximant R_3 under the conventional (Conv.) and the PMS scale settings. The *total*-column stands for the sum of all those loop corrections. $Q = 31.6$ GeV.

Given a perturbative series, it is important to know how well it behaves; *i.e.*, how much each loop term contributes. In Table III, we present the numerical results for the LO, NLO, N²LO and N³LO loop contributions to R_3 separately, in which the results for the conventional and the PMS scale settings are given. After applying the PMS, the magnitudes of the NLO, N²LO and N³LO loop-terms become much smaller than the corresponding ones under the conventional scale setting. This is due to the combined effect of the suppression of renormalon terms and the ‘‘induced convergence’’. However, this does not mean a more convergent pQCD series can be achieved. As shown by Table III, the pQCD series under the conventional scale setting has a standard perturbative convergence

$$|R_{3,\text{Conv.}}^{\text{LO}}| \gg |R_{3,\text{Conv.}}^{\text{NLO}}| > |R_{3,\text{Conv.}}^{\text{N}^2\text{LO}}| > |R_{3,\text{Conv.}}^{\text{N}^3\text{LO}}|,$$

which is mainly caused by α_s -power suppression. On the other hand, the PMS prediction shows a quite different perturbation series, *i.e.*,

$$R_{3,\text{PMS}}^{\text{LO}} \gg R_{3,\text{PMS}}^{\text{NLO}} \sim R_{3,\text{PMS}}^{\text{N}^2\text{LO}} \sim R_{3,\text{PMS}}^{\text{N}^3\text{LO}}$$

with $R_{3,\text{PMS}}^{\text{N}^2\text{LO}} > R_{3,\text{PMS}}^{\text{NLO}}$. The PMS prediction is determined by local RG-invariance, thus its goal is to achieve

¹ This property has been adopted for dealing with the coupling constant’s fixed-point behavior at the low-energy region [14, 15]. A detailed PMS analysis on physical observables at the low-energy region in comparison with those of PMC and conventional scale settings is in preparation [51].

the steady behavior of a perturbative series other than to improve its pQCD convergence. For example, the LO term $R_{3,\text{PMS}}^{\text{LO}}$ provides over 99% contributions to the PMS series, and the PMS prediction quickly approaches its steady behavior. However, its pQCD convergence can only be an accidental or it shall not show pQCD convergence at all.

	R_1	R_2	R_3	κ_1	κ_2	κ_3
Conv.	0.04786	0.04666	0.04635	7.44%	-2.50%	-0.66%
PMS	0.04889	0.04644	0.04638	9.76%	-5.00%	-0.14%

TABLE IV. Numerical results for R_n and κ_n with various QCD loop corrections under the conventional (Conv.) and PMS scale settings. The value of $R_0 = 0.04454$ is the same for both scale settings. $Q = 31.6$ GeV.

To show to what degree a low-order prediction can be improved by a high-order one, we define a ratio

$$\kappa_n = \frac{R_n - R_{n-1}}{R_{n-1}}, \quad n = (1, 2, 3)$$

To be a “convergent and accurate” $(n+1)$ -loop pQCD prediction, one would think that the magnitude of κ_n should be small enough and also be smaller than $\kappa_{(n-1)}$. Numerical results for R_n and κ_n up to four-loop level before and after the PMS scale setting are presented in Table IV. It shows that both conventional and PMS scale settings can give acceptable predictions when more high-order corrections have been taken into consideration. Up to four-loop level, the absolute values of κ_3 for the conventional and PMS scale settings are smaller than 1%, indicating that the pQCD predictions for this case are convergent and accurate enough; *i.e.*, the four-loop prediction R_3 are very close to the “true” value of the physical observable R . Following the trends of those predictions, we can expect that the physical value of R could be around 0.04635.

Previously, there was a doubt casted on the usefulness of PMS [19] for that it gives larger κ_1 and κ_2 than the conventional scale setting does. However the absolute value of PMS κ_3 is smaller than its counterpart of the conventional scale setting by about three times. This indicates that a larger PMS κ_1 and κ_2 only reflect the importance of N^3 -LO correction for PMS to achieving a better prediction than the conventional scale setting. Thus the available N^3 -LO correction helps us to clarify such kind of doubts on PMS.

It is helpful to find a way to predict “unknown” high-order pQCD corrections. Conventionally, this is done by varying the renormalization scale over a certain range, e.g. $\mu_0 \in [Q/2, 2Q]$. This conventional error estimate is not reliable, since it only partly estimates the high-order non-conformal contribution but not the more important conformal one [7]. It is no reason to choose 1/2 or 2 to discuss the error, why not 3 times or others? Moreover, for a scale setting such as PMS or PMC, it is unreasonable to simply vary their optimal scales via a similar

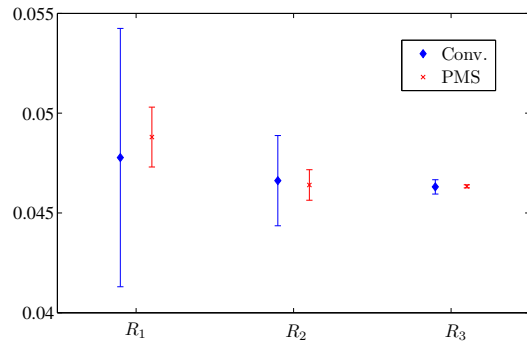


FIG. 1. Results for R_n ($n = 1, 2, 3$) together with their error estimates $(\pm |\tilde{\mathcal{C}}_n \tilde{a}_s^{n+1}|_{\text{MAX}})$. The diamonds and the crosses are for conventional (Conv.) and PMS scale settings, respectively. $Q = 31.6$ GeV.

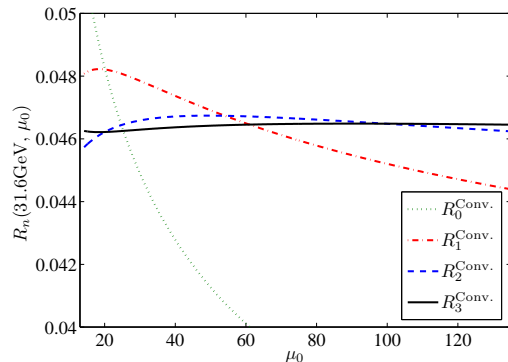


FIG. 2. The pQCD prediction $R_n^{\text{Conv.}}(Q = 31.6\text{GeV}, \mu_0)$ up to four-loop level versus the initial scale μ_0 . The dotted, the dash-dot, the dashed and the solid lines are for R_0 , R_1 , R_2 and R_3 , respectively.

way to predict “unknown” high-order pQCD corrections, since this way breaks the RG-invariance and leads to unreliable results. As a conservative prediction, one can take the perturbative uncertainty to be one of the last known order [13], *i.e.* the “unknown” high-order pQCD correction is taken as $(\pm |\mathcal{C}_n \tilde{a}_s^{n+1}|_{\text{MAX}})$ for a $(n+1)$ -loop prediction of R_n , where $|\mathcal{C}_n \tilde{a}_s^{n+1}|$ is calculated by varying $\mu_0 \in [Q/2, 2Q]$ ², and the symbol “MAX” stands for the maximum $|\mathcal{C}_n \tilde{a}_s^{n+1}|$ within this scale region. The error estimates for conventional and PMS scale settings are displayed in Fig.(1). It shows that the PMS errors are smaller than those under the conventional scale setting, which tend to shrink more rapidly with the increment of pQCD order. It is noted that the PMS R_2 and R_3 lie well outside the error estimation of R_1 . Thus the PMS

² As shown by the latter Fig.(3) the PMS prediction is independent to the choice of μ_0 , thus such choice of usual scale range only leads to a smaller conventional scale error.

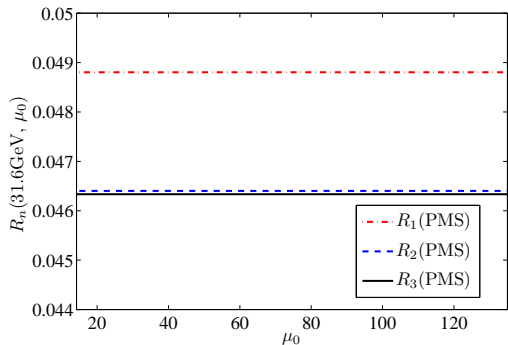


FIG. 3. The pQCD prediction $R_n^{\text{PMS}}(Q = 31.6\text{GeV}, \mu_0)$ up to four-loop level versus the initial scale μ_0 . The dash-dot, the dashed and the solid lines are for, R_1 , R_2 and R_3 , respectively.

prediction on R_1 along is not able to predict correct high-order contributions. Such an improper PMS prediction on R_1 also explains why PMS κ_1 and κ_2 are so large. However by including more high-order contributions, the PMS works better and gives more reliable predictions.

Finally, we discuss the scale dependence of R_n under different scale settings. We present the scale dependence of $R_n^{\text{Conv.}}(31.6\text{GeV}, \mu_0)$ up to four-loop level under the conventional scale setting in Fig.(2). The LO and NLO estimations, R_0 and R_1 , depend heavily on μ_0 . When more high-order corrections have been taken into account, the scale dependence becomes weaker. This agrees with the conventional wisdom that by computing high-order enough correction, one may get scale independent predictions. However, not all quantities in pQCD can be calculated to “accurate enough” high orders due to the complexity of high-loop QCD calculations. As a comparison, we present the scale dependence of $R_n^{\text{PMS}}(31.6\text{GeV})$ under the PMS scale setting in Fig.(3). It shows that the PMS does eliminate the initial scale dependence even for low fixed-order pQCD predictions, which is consistent with our previous conclusions drawn from the properties of RG-invariants.

B. R_τ up to four-loop level

The ratio for τ -lepton decays into hadrons is defined as

$$R_\tau = \frac{\Gamma(\tau \rightarrow \nu_\tau + \text{hadrons})}{\Gamma(\tau \rightarrow \nu_\tau + e^- \bar{\nu}_e)}, \quad (28)$$

which provides another fundamental test of pQCD and it can be calculated from $R_{e^+e^-}$ [55, 56]:

$$R_\tau(M_\tau) = 2 \int_0^{M_\tau^2} \frac{ds}{M_\tau^2} \left(1 - \frac{s}{M_\tau^2}\right)^2 \left(1 + \frac{2s}{M_\tau^2}\right) \tilde{R}_{e^+e^-}(\sqrt{s}).$$

Here $M_\tau = 1.777$ GeV [50] is the τ -lepton mass, s stands for the squared invariant mass of hadrons, and

$\tilde{R}_{e^+e^-}(\sqrt{s})$ can be obtained from $R_{e^+e^-}$ by replacing $3 \sum_q e_q^2$ with $3(|V_{ud}|^2 + |V_{us}|^2) \approx 3$.

After doing the integration over s and putting the explicit scale dependence into the expression, we can rewrite R_τ as

$$R_\tau(M_\tau, \mu_0) = 3(|V_{ud}|^2 + |V_{us}|^2)(1 + r_n^\tau(M_\tau, \mu_0)), \quad (29)$$

where the perturbative approximant

$$r_n^\tau(M_\tau, \mu_0) = \sum_{i=0}^n C'_i(M_\tau, \mu_0) a_s^{i+1}(\mu_0). \quad (30)$$

μ_0 stands for initial renormalization scale. At $\mu_0 = M_\tau$, the coefficients of R_τ under the $\overline{\text{MS}}$ -scheme up to four-loop level can be written as [21]

$$\begin{aligned} C'_0 &= 1, \\ C'_1 &= 6.3399 - 0.3791n_f, \\ C'_2 &= 48.5831 - 7.87865n_f + 0.15786n_f^2, \\ C'_3 &= 401.54 - 109.449n_f + 6.18148n_f^2 - 0.06366n_f^3. \end{aligned}$$

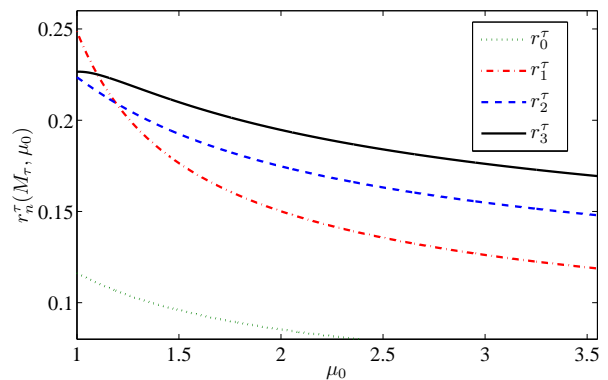


FIG. 4. The pQCD prediction $r_n^\tau(M_\tau, \mu_0)$ up to four-loop level versus the initial scale μ_0 under the conventional scale setting. The dotted, the dash-dot, the dashed and the solid lines are for r_0^τ , r_1^τ , r_2^τ and r_3^τ , respectively.

We start from the (initial) scale dependence of $r_n^\tau(M_\tau)$. The results for r_n^τ under the conventional scale setting are put in Fig.(4). It is found that the approximant r_n^τ strongly depends on μ_0 even for the four-loop prediction. This indicates that we need even more loop terms to make the final prediction accurate enough. On the other hand, after applying the PMS, we get the same initial scale independence at any orders as that of Fig.(3). In the following, we shall take $\mu_0 = M_\tau$ to do our discussions.

	C'_1	C'_2	C'_3
Conv.	5.2023	26.3659	127.079
PMS	0.3906	1.2380	-6.1747

TABLE V. Coefficients for the perturbative expansion of r_n^τ before and after the PMS scale setting. $\mu_0 = M_\tau$.

	$\tilde{a}_s^{(1)}$	$\tilde{a}_s^{(2)}$	$\tilde{a}_s^{(3)}$
Conv.	0.1042	0.1015	0.1032
PMS	0.4733	0.1963	0.1994

TABLE VI. The effective couplings $\tilde{a}_s^{(n)}$ for r_n^τ under the conventional (Conv.) and PMS scale settings. $\mu_0 = M_\tau$.

The coefficients \mathcal{C}'_n before and after the PMS scale setting are presented in Table V. Again the factorial renormalon growth of \mathcal{C}'_n has been suppressed. The effective couplings $\tilde{a}_s^{(n)}$ for r_n^τ under the conventional and PMS scale settings are presented in Table VI. In different to the case of R_n , there is no ‘‘induced convergence’’ for r_n^τ , i.e. $\tilde{a}_s^{(1)} > \tilde{a}_s^{(2)} \sim \tilde{a}_s^{(3)}$. Thus the ‘‘induced convergence’’ can only be an approximate property of PMS.

	LO	NLO	N ² LO	N ³ LO	total
Conv.	0.10320	0.05541	0.02898	0.01441	0.20200
PMS	0.19935	0.01552	0.00981	-0.00975	0.21493

TABLE VII. The LO, NLO, N²LO and N³LO loop contributions for the approximant r_3^τ under the conventional (Conv.) and the PMS scale settings. The *total*-column stands for the sum of all those loop corrections.

In Table VII, we present numerical results for the LO, NLO, N²LO and N³LO loop contributions to r_3^τ separately, in which the results for conventional and PMS scale settings are presented. The magnitude of N³-LO term under the conventional scale is about 7% of r_3^τ , which changes down to $\sim 4\%$ after applying PMS scale setting. The pQCD series under the conventional scale setting shows a standard perturbative convergence similar to the case of R_n . And the PMS prediction also shows a different perturbation series, *i.e.*,

$$r_{3,\text{PMS}}^{\tau,\text{LO}} \gg r_{3,\text{PMS}}^{\tau,\text{NLO}} > r_{3,\text{PMS}}^{\tau,\text{N}^2\text{LO}} \sim \left| r_{3,\text{PMS}}^{\tau,\text{N}^3\text{LO}} \right|$$

	r_1^τ	r_2^τ	r_3^τ	κ_1^τ	κ_2^τ	κ_3^τ
Conv.	0.16064	0.18255	0.20200	79.18%	13.64%	10.66%
PMS	0.36514	0.19781	0.21493	307.29%	-45.83%	8.66%

TABLE VIII. Numerical results for r_n^τ and κ_n^τ with various QCD loop corrections under the conventional (Conv.) and PMS scale settings. The value of $r_0^\tau = 0.0897$ is the same for both scale settings. $\mu_0 = M_\tau$.

Numerical results for r_n^τ and κ_n^τ under conventional and PMS scale settings are presented in Table VIII. The value of κ_3^τ under both scale settings are around 10%, indicating the necessity of calculating more high-order terms before an accurate pQCD prediction on R_τ can be achieved. κ_3^τ (PMS) is slightly smaller than κ_3^τ (Conv.), thus PMS can lead to relatively better four-loop prediction than the conventional scale setting. The PMS r_1^τ is

about 2.2 times larger than the conventional one, which provides the reason for large κ_1^τ and κ_2^τ .

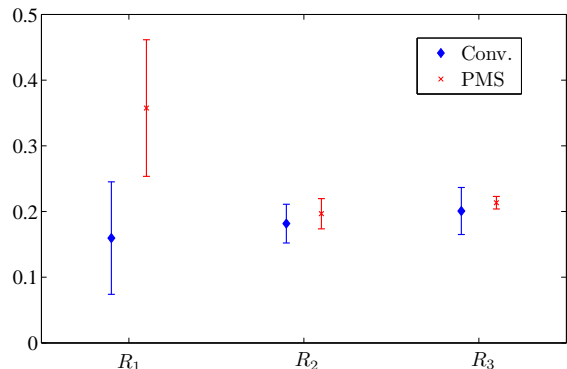


FIG. 5. Results for r_n^τ ($n = 1, 2, 3$) together with their errors ($\pm |\tilde{\mathcal{C}}'_n \tilde{a}_s^{n+1}|_{\text{MAX}}$). The diamonds and the crosses are for conventional scale setting (Conv.) and the PMS.

Results for r_n^τ ($n = 1, 2, 3$) together with their error estimates, *i.e.* the predicted unknown high-order contributions ($\pm |\tilde{\mathcal{C}}'_n \tilde{a}_s^{n+1}|_{\text{MAX}}$), are presented in Fig.(5). Similar to $R_{e^+e^-}$ case, $r_{2,3}^\tau$ are outside the prediction of r_1^τ . The PMS r_1^τ is even outside the conventional prediction of r_1^τ with large errors. Thus, the PMS prediction on r_1^τ along is not able to predict correct high-order contributions. But the PMS provides smaller errors for r_2^τ and r_3^τ than those given by the conventional method, and the PMS errors shrink quickly when more loop corrections are included. Using the four-loop prediction, we obtain

$$R_\tau(M, \mu_0)|_{\text{Conv.}} = 3.606 \pm 0.111, \quad (31)$$

$$R_\tau(M, \mu_0)|_{\text{PMS}} = 3.645 \pm 0.029. \quad (32)$$

where the errors are predicted high-order contributions for $\mu_0 \in [M/2, 2M]$. Both of them are consistent with the OPAL measurement [57], $R_\tau = 3.593 \pm 0.008$. These values strongly depends on the choice of $\Lambda_{\text{QCD}}^{n_f=3}$. Inversely, by using the OPAL data on R_τ and following the approach suggested in Ref.[13], we predict $\Lambda_{\text{Conv.}}^{n_f=3} = 340_{-5}^{+4}$ MeV and $\Lambda_{\text{PMS}}^{n_f=3} = 323_{-4}^{+4}$ MeV.

C. $\Gamma(H \rightarrow b\bar{b})$ up to four-loop level

The decay width for Higgs decaying into a $b\bar{b}$ pair can be written as

$$\Gamma(H \rightarrow b\bar{b}) = \frac{3G_F M_H m_b^2(M_H)}{4\sqrt{2}\pi} (1 + \tilde{R}_n), \quad (33)$$

where G_F is the Fermi constant, M_H is the mass of Higgs Boson, $m_b(M_H)$ is the b -quark $\overline{\text{MS}}$ running mass, and up to $(n+1)$ -loop level, we have

$$\tilde{R}_n(M_H, \mu_0) = \sum_{i=0}^n \tilde{\mathcal{C}}'_i(M_H, \mu_0) a_s^{i+1}(\mu_0),$$

where μ_0 stands for an arbitrary initial scale. The QCD corrections for the decay width $\Gamma(H \rightarrow b\bar{b})$ have been calculated up to four-loop level, cf. Refs.[23, 24, 58, 59];

$$\begin{aligned} \tilde{R}_3 = & 5.6667a_s(M_H) + (35.94 - 1.359n_f)a_s^2(M_H) + (164.14 - 25.77n_f + 0.259n_f^2)a_s^3(M_H) \\ & + (39.34 - 220.9n_f + 9.685n_f^2 - 0.0205n_f^3)a_s^4(M_H). \end{aligned} \quad (34)$$

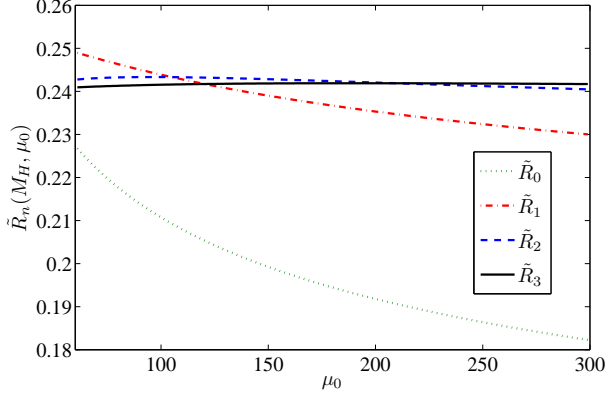


FIG. 6. The pQCD prediction $\tilde{R}_n(M_H, \mu_0)$ up to four-loop level versus the initial scale μ_0 under the conventional scale setting. The dotted, the dash-dot, the dashed and the solid lines are for \tilde{R}_0 , \tilde{R}_1 , \tilde{R}_2 , and \tilde{R}_3 , respectively.

The initial scale dependence of \tilde{R}_n under conventional scale setting is presented in Fig.(6). The scale dependence becomes weaker with the increment of high-loop terms, and the four-loop prediction \tilde{R}_3 is almost independent to the scale changes. This is the standard properties of pQCD prediction from the conventional scale setting, which however can not weaken the importance of a more proper scale setting. For example, after applying the PMS, we get the same initial scale independence at lower orders as the same as those of Fig.(3).

	C_1''	C_2''	C_3''
Conv.	29.145	41.765	-825.598
PMS	0.34376	21.2286	-142.849

TABLE IX. Coefficients for the perturbative expansion of \tilde{R}_3 before and after the PMS scale setting. $\mu_0 = M_H$.

	$\tilde{a}_s^{(1)}$	$\tilde{a}_s^{(2)}$	$\tilde{a}_s^{(3)}$
Conv.	0.0360	0.0360	0.0359
PMS	0.0465	0.0425	0.0423

TABLE X. The effective couplings $\tilde{a}_s^{(n)}$ for \tilde{R}_n under the conventional (Conv.) and PMS scale settings. $\mu_0 = M_H$.

For $\mu_0 = M_H$, the four-loop \tilde{R}_3 reads [23]

The coefficients C_n'' before and after PMS scale setting in Table IX. Because of the renormalon term, the absolute value of $C_3'' \sim 826$, which changes down to ~ 143 by applying PMS. The effective couplings $\tilde{a}_s^{(n)}$ for \tilde{R}_n under conventional (Conv.) and PMS scale settings are presented in Table X. For the present case, the effective couplings \tilde{a}_s for conventional scale setting are almost unchanged, while the PMS ones decreases with the increment of loop-terms.

	LO	NLO	N ² LO	N ³ LO	total
Conv.	0.20371	0.03767	0.00194	-0.00138	0.24194
PMS	0.23967	0.00061	0.00161	-0.00046	0.24144

TABLE XI. The LO, NLO, N²LO and N³LO loop contributions for the approximant \tilde{R}_3 under the conventional (Conv.) and the PMS scale settings. The *total*-column stands for the sum of all those loop corrections. $\mu_0 = M_H$.

The LO, NLO, N²LO and N³LO loop contributions for the approximant \tilde{R}_3 under conventional (Conv.) and PMS scale settings are presented in Table XI. The LO term provides dominant contribution to \tilde{R}_3 . The magnitude of N³-LO term under conventional scale setting provides a smaller $\sim 0.6\%$ contribution to \tilde{R}_3 , which changes down to 0.2% after applying PMS scale setting. The pQCD series under conventional scale setting shows a standard perturbative convergence similar to the case of R_n . And the PMS prediction also shows a different perturbation series, *i.e.*,

$$\tilde{R}_{3,\text{PMS}}^{\text{LO}} \gg \tilde{R}_{3,\text{PMS}}^{\text{NLO}}, \tilde{R}_{3,\text{PMS}}^{\text{N}^2\text{LO}}, \tilde{R}_{3,\text{PMS}}^{\text{N}^3\text{LO}}$$

with $\tilde{R}_{3,\text{PMS}}^{\text{N}^2\text{LO}} > \tilde{R}_{3,\text{PMS}}^{\text{NLO}}$.

	\tilde{R}_1	\tilde{R}_2	\tilde{R}_3	$\tilde{\kappa}_1$	$\tilde{\kappa}_2$	$\tilde{\kappa}_3$
Conv.	0.24151	0.24333	0.24194	18.28%	0.75%	-0.57%
PMS	0.25621	0.24087	0.24144	25.48%	-5.99%	0.24%

TABLE XII. Numerical results for \tilde{R}_n and $\tilde{\kappa}_n$ with various QCD loop corrections under the conventional (Conv.) and PMS scale settings. The value of $\tilde{R}_0 = 0.20419$ is the same for both scale settings. $\mu_0 = M_H$.

Numerical results for \tilde{R}_n and $\tilde{\kappa}_n$ up to four-loop level are presented in Table XII. Results for \tilde{R}_n ($n = 1, 2, 3$)

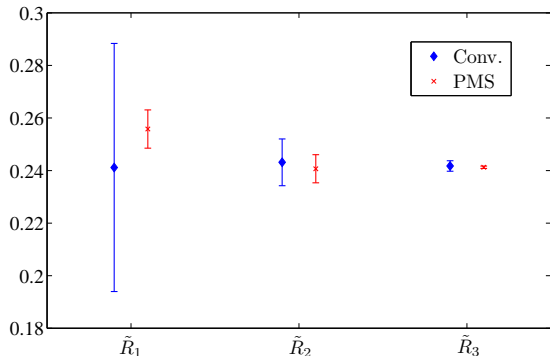


FIG. 7. Results for \tilde{R}_n ($n = 1, 2, 3$) together with their prediction of unknown high-order contributions ($\pm|\tilde{C}_n''\tilde{a}_s^{n+1}|_{\text{MAX}}$) for $H \rightarrow b\bar{b}$. The diamonds and the crosses are for conventional (Conv.) and PMS scale settings, respectively.

together with their prediction of unknown high-order contributions ($\pm|\tilde{C}_n''\tilde{a}_s^{n+1}|_{\text{MAX}}$) are presented in Fig.(7). The four-loop \tilde{R}_3 are nearly the same for conventional and PMS scale settings; while the PMS $\tilde{\kappa}_3$ is smaller and is more close to its final prediction on the observable \tilde{R} . However, the PMS \tilde{R}_1 also can not predict the correct high-order contributions, i.e. both \tilde{R}_2 and \tilde{R}_3 are outside its prediction. Such larger PMS \tilde{R}_1 also leads to larger $\tilde{\kappa}_1$ and $\tilde{\kappa}_2$. With those \tilde{R}_3 results, we present the decay width of Higgs into a $b\bar{b}$ pair:

$$\Gamma(H \rightarrow b\bar{b})|_{\text{Conv.}} = 2389.85 \pm 3.85 \text{ KeV}, \quad (35)$$

$$\Gamma(H \rightarrow b\bar{b})|_{\text{PMS}} = 2388.87 \pm 0.88 \text{ KeV}, \quad (36)$$

where the errors are predicted unknown high-order contributions for $\mu_0 \in [M_H/2, 2M_H]$.

IV. A COMPARISON OF PMS AND PMC

The running behavior of the coupling constant is controlled by the RG-equation. In different to the local RG-invariance of PMS, the PMC [26–32] respects the standard RG-invariance and improves the perturbative series by absorbing all β -terms governed by RG-equation into the coupling constant. The PMC procedure can be advantageously applied to entire range of perturbatively calculable QCD and Standard Model processes. Recently, many high-order PMC applications have been finished and the PMC works successfully, cf.Refs.[60–64]. It is helpful to present a detailed comparison of PMS and PMC predictions. For the purpose, we take $R_{e^+e^-}$ as an explicit example.

After applying the PMC, the coefficients C_n^{PMC} for R_3 are presented in Table XIII. Comparing with Table I, PMC coefficients are smaller than the conventional ones. PMS also leads to such a suppression, but it can not explain why. PMC shows that such suppression are rightly

	$n_f=3$	$n_f=4$	$n_f=5$
C_1^{PMC}	2.14579	1.99302	1.84024
C_2^{PMC}	3.39697	1.21574	-1.00503
C_3^{PMC}	6.47103	-12.8517	-11.0871

TABLE XIII. Coefficients C_n^{PMC} for the perturbative expansion of $R_3(Q)$ using the PMC scale setting, where we have set $Q = 1.2 \text{ GeV}$ for $n_f=3$, $Q = 3 \text{ GeV}$ for $n_f=4$, and $Q = 31.6 \text{ GeV}$ for $n_f=5$.

due to the elimination of renormalon terms.

	R_1	R_2	R_3	κ_1	κ_2	κ_3
PMS	0.04889	0.04644	0.04638	9.76%	-5.00%	-0.14%
PMC	0.04767	0.04667	0.04635	7.03%	-2.09%	-0.69%

TABLE XIV. A comparison of R_n and κ_n under the PMS and PMC scale settings. The value of $R_0 = 0.04454$ is the same for both scale settings. $Q = 31.6 \text{ GeV}$ and $\mu_0 = Q$.

A comparison of R_n and κ_n under PMS and PMC scale settings is presented in Table XIV. The differences for three-loop R_2 is about 0.5%, which moves down to about 0.05% for four-loop R_3 . Both PMS and PMC are based on RG-invariance, it is reasonable that they can give close numerical predictions at higher orders. The values of PMC κ_1 and κ_2 are smaller than PMS, indicating a faster steady behavior can be achieved by PMC³.

	LO	NLO	N ² LO	N ³ LO	total
PMS	0.04608	0.00010	0.00013	0.00007	0.04638
PMC	0.04290	0.00351	-0.00004	-0.00002	0.04635

TABLE XV. The LO, NLO, N²LO and N³LO loop contributions for the approximant R_3 under the PMS and PMC scale settings. The *total*-column stands for the sum of all those loop corrections. $Q = 31.6 \text{ GeV}$ and $\mu_0 = Q$.

A comparison of PMS and PMC pQCD series is presented in Table XV. The PMC pQCD series follows the standard pQCD convergence but is much more convergent than that of conventional scale setting; while, the PMS series also becomes more convergent than the conventional ones, but the series does not show the order-by-order convergence, i.e. $R_{3,\text{PMS}}^{\text{N}^2\text{LO}} > R_{3,\text{PMS}}^{\text{NLO}}$.

In Fig.(8), we present a comparison of PMC and PMS predictions for R_n ($n = 1, 2, 3$) together with their predicted unknown high-order contributions ($\pm|\tilde{C}_n''\tilde{a}_s^{n+1}|_{\text{MAX}}$). The large error bar for PMC R_1 shows the magnitude of the NLO-conformal terms are large and

³ The PMS κ_3 for $R_{e^+e^-}$ is accidentally small. We have found that PMC κ_3 for R_τ and $\Gamma(H \rightarrow b\bar{b})$ are smaller than those of PMS, following the same trends.

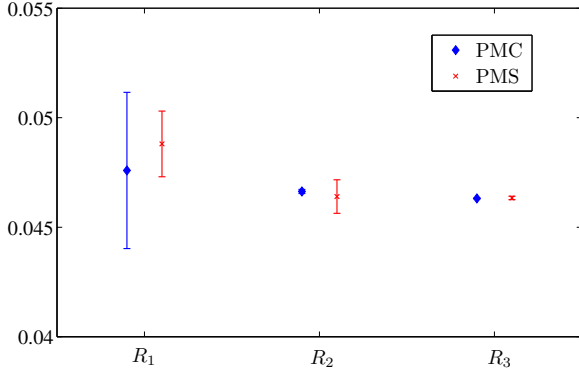


FIG. 8. A comparison of PMC and PMS predictions for R_n ($n = 1, 2, 3$) together with their predicted unknown high-order contributions ($\pm|\tilde{\mathcal{C}}_n \tilde{a}_s^{n+1}|_{\text{MAX}}$). The diamonds and the crosses are for PMC and PMS scale settings, respectively.

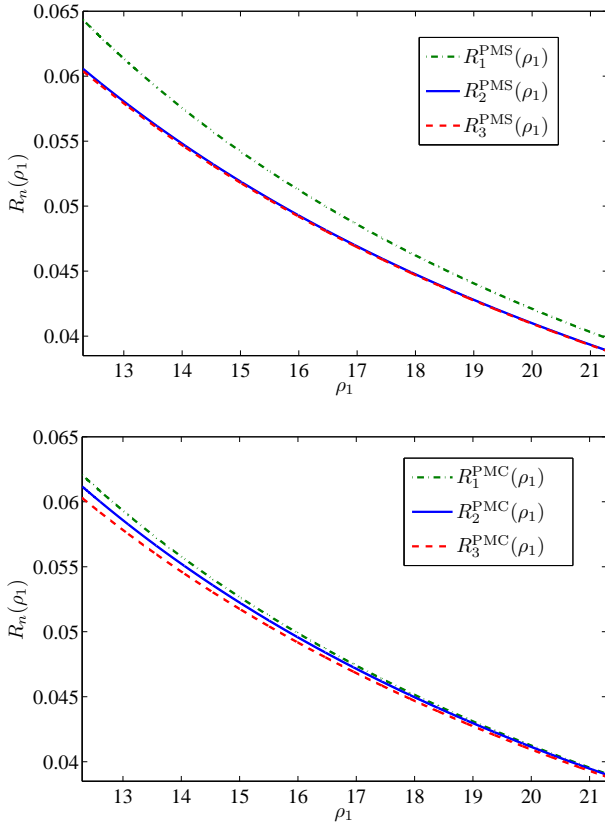


FIG. 9. The curves of the function $R_n(\rho_1)$ for the PMS and PMC scale settings. $\mu_0 = Q$.

we need even high-order terms to achieve an accurate prediction. In fact, when we have more β -terms to fix the PMC scales, the PMC prediction together with its predicted error does become more accurate.

	δ_1	δ_2	δ_3
Conv.	2.24%	0.55%	0.10%
PMC	2.66%	0.61%	0.07%

TABLE XVI. The difference δ_n for $R_n(\rho_1)$ between the PMC (or conventional) scale setting and the PMS scale setting.

We present a comparison of PMS and PMC energy dependence of $R_n(Q)$ in Fig.(9), where we have changed the argument to ρ_1 such that to avoid the uncertainty from Λ_{QCD} [20]. The present range $\rho_1 \in (12, 21)$ corresponds to energy range $9 < Q < 90$ GeV. There is large difference between $R_1^{\text{PMS}}(\rho_1)$ and $R_{n \geq 2}^{\text{PMS}}(\rho_1)$, which is consistent with previous observation that $R_1^{\text{PMS}}(\rho_1)$ along can not predict reasonable unknown high-order contributions. To show the difference of the predicted $R_n(\rho_1)$ under various scale settings more accurately, we define a parameter, δ_n , as

$$\delta_n = \frac{\sum_{\rho_1} |R_n(\rho_1) - R_n^{\text{PMS}}(\rho_1)|}{\sum_{\rho_1} |R_n^{\text{PMS}}(\rho_1)|} \times 100\%, \quad (37)$$

where $\rho_1 = 12, 12.001, 12.002, \dots, 21$. Those differences are presented in Table XVI. The differences of $R_n(\rho_1)$ among different scale settings shall be reduced with more loop corrections being included.

V. SUMMARY

To solve the renormalization scheme and renormalization scale ambiguities, one should answer the question of how to set optimal scale systematically for any physical processes up to any orders from some basic principal of QCD theory. As a practical solution, the PMS adopts local RG-invariance (7,8) to set the optimal scheme and optimal scale of the process.

Based on the local RG-invariance, we have presented the detailed technology for applying PMS to high-perturbative orders. We have investigated the PMS properties based on three typical physical quantities $R_{e^+e^-}$, R_τ and $\Gamma(H \rightarrow b\bar{b})$ up to four-loop QCD corrections. Our analysis show that even though the PMS is theoretically unsound, it does provide an effective approach to soften the renormalization scheme and scale ambiguities by including enough higher-order pQCD contributions. More explicitly, our results show that

- After applying the PMS, the magnitudes of perturbative coefficients become smaller than those under conventional scale setting, indicating the divergent renormalon terms can be suppressed. The PMS effective coupling approximately satisfies the “induced convergence”. As a combined effect, the magnitudes of NLO and higher-order loop-terms become much smaller than the corresponding ones under conventional scale setting.

- The goal of PMS is to achieve the steady point of a perturbative series over the renormalization scheme and scale changes. The PMS predictions for those three four-loop examples do show such a steady behavior, i.e. the final PMS predictions are independent of any choice of initial scale, being consistent with one of requirement of basic RG-invariance. Moreover, the LO terms $R_{3,\text{PMS}}^{\text{LO}}$ and $\tilde{R}_{3,\text{PMS}}^{\text{LO}}$ provide $\sim 99\%$ contributions, and $r_3^{\tau,\text{LO}}$ provides $\sim 89\%$ contribution to $R_{e^+e^-}$, $\Gamma(H \rightarrow b\bar{b})$ and R_τ series, respectively. However, the PMS have no principal to ensure the pQCD convergence, thus the improved pQCD convergence for some of the high-energy processes could only be an accidental. In fact, all those three four-loop examples do not have standard pQCD convergence, i.e. the magnitudes of their NLO, N²LO and N³LO terms are usually small but at the same order.
- We have suggested a conservative way to discuss the pQCD predictive power, i.e. to show how unknown high-order terms contribute. It is noted that after PMS scale setting, the N²LO and N³LO estimates are usually outside the predicted errors by using the terms only up to NLO level. Together with other lower-order PMS behaviors, such as the large PMS $\kappa_{1,2}$ for the mentioned processes, we may conclude that PMS can not provide correct lower-order predictions, such as the NLO predictions. In the literature, most of the doubts on PMS are rightly based on lower-order predictions. With more loop corrections being included, the PMS can achieve a more accurate prediction better than that of conventional scale setting.

In the paper, we have also presented a comparison of PMS and PMC predictions. In different to PMS, the PMC satisfies standard RG-invariance and follows the RG-equation to fix the running behavior of the coupling constant, thus it is theoretical sound. The PMC predictions have optimal pQCD convergence due to the elimination of renormalon terms. The PMS prediction is independent on the choice of initial scale; while there is residual scale dependence for PMC predictions due to unknown high-order β -term, however such residual scale de-

pendence is highly suppressed, even for lower-order PMC predictions. In comparison to the conventional and PMS scale settings, the PMC shows a better predictive power, and its predictions quickly approaches the physical value of the observable. Moving to high-order pQCD predictions, the PMS and PMC differences on the pQCD predictions shall be greatly suppressed, e.g. for the case of $R_{e^+e^-}$, the differences change from larger $\sim 3\%$ at the NLO level, to be $\sim 1\%$ at the N²LO level, and to be less than 0.1% at the N³-LO level.

Acknowledgments: We thank Stanley J. Brodsky, Hai-Bing Fu, Matin Mojaza, Paul M. Stevenson, Sheng-Quan Wang, and Xu-Chang Zheng for helpful discussions. This work was supported in part by Natural Science Foundation of China under Grant No.11275280, by the Fundamental Research Funds for the Central Universities under Grant No.CQDXWL-2012-Z002.

Appendix A: A tricky way to derive the RG-invariants ρ_n at high-orders

In this appendix, we present a simpler way to drive the RG-invariants ρ_n at high-orders with $n > 1$, basing on their properties of RG-invariance.

For convenience, we set $p = 1$ in Eq.(3) and redefine the $\beta^{\mathcal{R}}$ -function as

$$\beta^{\mathcal{R}} = \mu^2 \frac{\partial}{\partial \mu^2} \left(\frac{\alpha_s(\mu)}{4\pi} \right) = - \sum_{i=0}^{\infty} b_i a_s^{i+2}, \quad (\text{A1})$$

where $b_i = (1/4)^{i+2} \beta_i^{\mathcal{R}}$ and $a_s = \alpha_s/\pi$.

A physical observable solitarily defines an effective charge [65–67], and vice versa. Thus, we can inversely write down the coupling constant a_s as an expression over the approximant ϱ_n [68], i.e.

$$a_s(\varrho_n) = \varrho_n + \sum_{i=1}^{\infty} r_i \varrho_n^{i+1} \quad (\text{A2})$$

Substituting the ϱ_n expression (3) into Eq.(A2), we obtain

$$a_s = a_s (1 + \mathcal{C}_1 a_s + \mathcal{C}_2 a_s^2 + \mathcal{C}_3 a_s^3 + \dots) [1 + r_1 a_s (1 + \mathcal{C}_1 a_s + \mathcal{C}_2 a_s^2 + \mathcal{C}_3 a_s^3 + \dots) + r_2 a_s^2 (1 + \mathcal{C}_1 a_s + \mathcal{C}_2 a_s^2 + \mathcal{C}_3 a_s^3 + \dots)^2 + \dots] \quad (\text{A3})$$

$$= a_s [1 + a_s (r_1 + \mathcal{C}_1) + a_s^2 (2r_1 \mathcal{C}_1 + r_2 + \mathcal{C}_2) + a_s^3 (r_1 \mathcal{C}_1^2 + 2r_1 \mathcal{C}_2 + 3r_2 \mathcal{C}_1 + r_3 + \mathcal{C}_3) + \dots], \quad (\text{A4})$$

where the symbol \dots stands for higher-order terms. The coefficients for a_s^2 and higher orders should vanish, which

lead to

$$r_1 = -\mathcal{C}_1, \quad (\text{A5})$$

$$r_2 = 2\mathcal{C}_1^2 - \mathcal{C}_2, \quad (\text{A6})$$

$$r_3 = \mathcal{C}_1^3 - 3(2\mathcal{C}_1^2 - \mathcal{C}_2)\mathcal{C}_1 + 2\mathcal{C}_1 \mathcal{C}_2 - \mathcal{C}_3 \quad (\text{A7})$$

\vdots

As a further step, we introduce a new function

$$\mathcal{R}(Q) = \frac{\partial}{\partial \ln Q^2} \varrho_n(Q) = 4\beta^{\mathcal{R}} \frac{\partial}{\partial a_s(Q)} \varrho_n(Q), \quad (\text{A8})$$

where Q is the scale at which the observable is measured.

$$\begin{aligned} \mathcal{R} = & -\varrho_n^2 [4b_0 + 4\varrho_n(2r_1b_0 + b_1 + 2\mathcal{C}_1b_0) + 4\varrho_n^2(r_1^2b_0 + 3r_1b_1 + 6r_1b_0\mathcal{C}_1 + 2r_2b_0 + b_2 + 3b_0\mathcal{C}_2 + 2b_1\mathcal{C}_1) \\ & + 4\varrho_n^3(2r_1r_2b_0 + 2r_3b_0 + 3r_1^2b_1 + 3r_2b_1 + 4r_1b_2 + b_3 + 6r_1^2b_0\mathcal{C}_1 + 6r_2b_0\mathcal{C}_1 + 8r_1b_1\mathcal{C}_1 + 2b_2\mathcal{C}_1 \\ & + 12r_1b_0\mathcal{C}_2 + 3b_1\mathcal{C}_2 + 4b_0\mathcal{C}_3) + \dots] \quad (\text{A9}) \\ = & -\varrho_n^2 [4b_0 + 4\varrho_n b_1 + 4\varrho_n^2(b_2 - b_0\mathcal{C}_1^2 - b_1\mathcal{C}_1 + b_0\mathcal{C}_2) + 4\varrho_n^3(4b_0\mathcal{C}_1^3 - 6b_0\mathcal{C}_1\mathcal{C}_2 + 2b_0\mathcal{C}_3 + b_1\mathcal{C}_1^2 - 2b_2\mathcal{C}_1 + b_3) + \dots] \quad (\text{A10}) \end{aligned}$$

Both ϱ_n and \mathcal{R} are physical quantities, the expansion coefficients of \mathcal{R} over ϱ_n should be RG invariants. Transforming these RG invariant coefficients back into the notation used in the body of the text, we get the RG in-

Since ϱ_n and Q are physical quantities, \mathcal{R} can also be regarded as a physical quantity that does not depend on the renormalization scheme and scale. Eq.(A8) can be expanded over ϱ_n in the following form,

variants ρ_n ($n > 1$). The first two of them are

$$\rho_2 = \frac{\beta_2}{16\beta_0} - \frac{\beta_1\mathcal{C}_1}{4\beta_0} - \mathcal{C}_1^2 + \mathcal{C}_2, \quad (\text{A11})$$

$$\rho_3 = \frac{\beta_3}{64\beta_0} + \frac{\beta_1\mathcal{C}_1^2}{4\beta_0} - \frac{\beta_2\mathcal{C}_1}{8\beta_0} + 4\mathcal{C}_1^3 - 6\mathcal{C}_2\mathcal{C}_1 + 2\mathcal{C}_3 \quad (\text{A12})$$

Finally, by replacing ϱ_n to $\varrho_n^{\frac{1}{p}}$, we can obtain the RG-invariants for any p . The first two of which agree with Eqs.(22,24).

-
- [1] E.C.G. Stueckelberg and A. Peterman, *Helv. Phys. Acta.* **26**, 499 (1953).
[2] M. Gell-Mann and F.E. Low, *Phys. Rev.* **95**, 1300 (1954).
[3] N.N. Bogoliubov and D.V. Shirkov, *Dokl. Akad. Nauk SSSR* **103**, 391 (1955).
[4] C.G. Callan, *Phys. Rev. D* **2**, 1541 (1970).
[5] K. Symanzik, *Commun. Math. Phys.* **18**, 227 (1970).
[6] A. Peterman, *Phys. Rep.* **53**, 157 (1979).
[7] X.G. Wu, S.J. Brodsky, and M. Mojaza, *Prog. Part. Nucl. Phys.* **72**, 44 (2013).
[8] P.M. Stevenson, *Phys. Rev. D* **23**, 2916 (1981).
[9] P.M. Stevenson, *Phys. Lett. B* **100**, 61 (1981).
[10] P.M. Stevenson, *Nucl. Phys. B* **203**, 472 (1982).
[11] J. Chyla, A.L. Kataev and S.A. Larin, *Phys. Lett. B* **267**, 269 (1991).
[12] S.G. Gorishnii, A.L. Kataev, S.A. Larin and L.R. Surguladze, *Phys. Rev. D* **43**, 1633 (1991).
[13] X.G. Wu, Y. Ma, S.Q. Wang, H.B. Fu, H.H. Ma, S.J. Brodsky, and M. Mojaza, arXiv:1405.3196.
[14] A.C. Mattingly and P.M. Stevenson, *Phys. Rev. D* **49**, 437 (1994).
[15] P.M. Stevenson, *Nucl. Phys. B* **875**, 63 (2013).
[16] S.J. Brodsky and X.G. Wu, *Phys. Rev. D* **86**, 054018 (2012).
[17] G. Kramer and B. Lampe, *Z. Phys. C* **39**, 101 (1988).
[18] G. Kramer and B. Lampe, *Z. Phys. A* **339**, 189 (1991).
[19] A.P. Contogouris and N. Mebarki, *Phys. Rev. D* **39**, 1464 (1989).
[20] P.M. Stevenson, *Nucl. Phys. B* **868**, 38 (2013).
[21] P.A. Baikov, K.G. Chetyrkin, and J.H. Kuhn, *Phys. Rev. Lett.* **101**, 012002 (2008).
[22] P.A. Baikov, K.G. Chetyrkin, and J.H. Kuhn, *Nucl. Phys. Proc. Suppl.* **189**, 49 (2009).
[23] P. A. Baikov, K. G. Chetyrkin, and J. H. Kuhn, *Phys. Rev. Lett.* **96**, 012003 (2006).
[24] P.A. Baikov and K.G. Chetyrkin, *Phys. Rev. Lett.* **97**, 061803 (2006).
[25] S.J. Brodsky, G.P. Lepage, and P.B. Mackenzie, *Phys. Rev. D* **28**, 228 (1983).
[26] S.J. Brodsky and X.G. Wu, *Phys. Rev. D* **85**, 034038 (2012).
[27] S.J. Brodsky and X.G. Wu, *Phys. Rev. D* **85**, 114040 (2012).
[28] S.J. Brodsky and X.G. Wu, *Phys. Rev. D* **86**, 014021 (2012).
[29] S.J. Brodsky and X.G. Wu, *Phys. Rev. Lett.* **109**, 042002 (2012).
[30] S.J. Brodsky and L.D. Giustino, *Phys. Rev. D* **86**, 085026 (2012).
[31] M. Mojaza, S.J. Brodsky, and X.G. Wu, *Phys. Rev. Lett.* **110**, 192001 (2013).
[32] S.J. Brodsky, M. Mojaza, and X.G. Wu, *Phys. Rev. D* **89**, 014027 (2014).
[33] S.J. Brodsky and H.J. Lu, *Phys. Rev. D* **51**, 3652 (1995).
[34] H.D. Politzer, *Phys. Rev. Lett.* **30**, 1346 (1973).
[35] D. Gross and F. Wilczek, *Phys. Rev. Lett.* **30**, 1343 (1973).
[36] O.V. Tarasov, A.A. Vladimirov, and A. Yu Zharkov, *Phys. Lett. B* **93**, 429 (1980).
[37] S.A. Larin and J.A.M. Vermaseren, *Phys. Lett. B* **303**, 334 (1993).
[38] T. van Ritbergen, J.A.M. Vermaseren, and S.A. Larin,

- Phys. Lett. B **400**, 379 (1997).
- [39] K.G. Chetyrkin, Nucl. Phys. B **710**, 499 (2005).
 - [40] M. Czakon, Nucl. Phys. B **710**, 485 (2005).
 - [41] D.J. Gross and A. Neveu, Phys. Rev. D **10**, 3235 (1974).
 - [42] B. Lautrup, Phys. Lett. B **69**, 109 (1977).
 - [43] R. Shrock, Phys. Rev. D **88**, 036003 (2013)
 - [44] R. Shrock, Phys. Rev. D **90**, 045011 (2014).
 - [45] G. Choi and R. Shrock, arXiv:1411.6645.
 - [46] H.J. Lu and S.J. Brodsky, Phys. Rev. D **48**, 3310 (1993).
 - [47] P.M. Stevenson, Phys. Rev. D **33**, 3130 (1986).
 - [48] A.C. Mattingly and P.M. Stevenson, Phys. Rev. Lett. **69**, 1320 (1992).
 - [49] A.C. Mattingly and P.M. Stevenson, Phys. Rev. D **49**, 437 (1994).
 - [50] K.A. Olive *et al.* (Particle Data Group). Chin. Phys. C **38**, 090001 (2014).
 - [51] Y. Ma *et al.*, in preparation.
 - [52] P.M. Stevenson, Nucl. Phys. B **231**, 65 (1984).
 - [53] W.E. Caswell, Ann. Phys. **123**, 153 (1979).
 - [54] R. Marshall, Z. Phys. C **43**, 595 (1989).
 - [55] C.S. Lam and T.M. Yan, Phys. Rev. D **16**, 703 (1977).
 - [56] E. Braaten, Phys. Rev. D **39**, 1458 (1989).
 - [57] K. Ackerstaff *et al.* (OPAL Collaboration), Eur. Phys. J. C **7**, 571 (1999).
 - [58] K.G. Chetyrkin, Phys. Lett. B **390**, 309 (1997).
 - [59] K.G. Chetyrkin and M. Steinhauser, Phys. Lett. B **408**, 320 (1997).
 - [60] S.Q. Wang, X.G. Wu, X.C. Zheng, J.M. Shen, and Q.L. Zhang, Eur. Phys. J. C **74**, 2825 (2014).
 - [61] S.Q. Wang, X.G. Wu, X.C. Zheng, G. Chen, and J.M. Shen, J. Phys. G **41**, 075010 (2014).
 - [62] S.Q. Wang, X.G. Wu, J.M. Shen, H.Y. Han, and Y. Ma, Phys. Rev. D **89**, 116001 (2014).
 - [63] S.Q. Wang, X.G. Wu, and S.J. Brodsky, Phys. Rev. D **90**, 037503 (2014).
 - [64] S.Q. Wang, X.G. Wu, Z.G. Si, and S.J. Brodsky, Phys. Rev. D **90**, 114034 (2014).
 - [65] G. Grunberg, Phys. Lett. B **95**, 70 (1980).
 - [66] G. Grunberg, Phys. Lett. B **110**, 501 (1982).
 - [67] G. Grunberg, Phys. Rev. D **29**, 2315 (1984).
 - [68] C.J. Maxwell, Phys. Rev. D **29**, 2884 (1984).